Radiation Measurements 144 (2021) 106592

Contents lists available at ScienceDirect

Radiation Measurements

journal homepage: www.elsevier.com/locate/radmeas

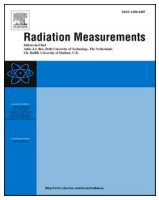

Assessment of secondary neutrons from galactic cosmic rays at mountain altitudes – Geant4 simulations and ground-based measurements of neutron energy spectra

T. Brall [a,*], V. Mares [a], R. Bütikofer [b], W. Rühm [a]

[a] Helmholtz Zentrum München, Institute of Radiation Medicine, Ingolstädter Landstr. 1, 85764 Neuherberg, Germany
[b] University of Bern, Space Research & Planetary Sciences, Sidlerstrasse 5, 3012 Bern, Switzerland

A B S T R A C T

In this study, the Geant4 Monte Carlo toolkit was used to simulate energy spectra of neutrons from secondary cosmic radiation at mountain altitudes for the Environmental Research Station "Schneefernerhaus" at the Zugspitze mountain, Germany (2660 m a.s.l.) and for Sphinx astronomical observatory at the Jungfraujoch, Switzerland (3585 m a.s.l.). Simulations were performed with different intra-nuclear cascade models available in Geant4, and the results were compared with those of measurements that had been performed at both locations by means of an Extended-Range Bonner Sphere Spectrometer. Measurement conditions were quite different for both locations – at Schneefernerhaus the measurements had been performed on the flank of a hill in March 2018 with much snow, while at Jungfraujoch the measurements had been performed on top of a steep local hill in September 2018 with much less snow. Despite these differences, agreement between measurement and simulation was reasonable at both locations, especially at neutron energies greater than 20 MeV where the (unknown) hydrogen content of the environment did not influence the neutron fluence much (i.e., results from simulations were 6–22% lower than those from the measurements for the Schneefernerhaus, and were 22–29% lower for Jungfraujoch, depending on intra-nuclear model used in the simulations). The agreement was less favorable for lower energies, where environmental hydrogen (e.g., snow cover, soil moisture) is known to influence the shape of the neutron energy spectrum, because the real conditions of the snow accumulation close to the location of the measurements were not known and, therefore, a detailed description of the real hydrogen environment in the simulations was not possible. When the results simulated using different intra-nuclear cascade models were compared with each other, agreement was found within ±5%, ±15%, ±20%, and ±20%, for cascade, evaporation, epithermal and thermal neutrons, respectively. While the latter results are consistent with those of simulations and measurements at the CERN EU High-Energy Reference Field (CERF) facility published recently, a detailed sensitivity analysis of the influence of environmental hydrogen on neutron energy spectra is required before a final quantitative comparison of measurements and simulations can be made. This sensitivity analysis is presently under way. It is concluded that simulation of energy spectra of neutrons from secondary cosmic rays close to the atmosphere-lithosphere interface, validated by the spectrometer measurements, showed differences of less than 30%, for neutron energies greater than 20 MeV, whatever intra-nuclear cascade model was used in the simulations.

1. Introduction

The Earth is continuously exposed to high-energy particles from the galactic space – so-called galactic cosmic rays (GCRs). When these primary GCR particles enter the Earth's atmosphere they interact with the atmosphere and generate a complex field of secondary particles including neutrons. Composition and intensity of this field depend on the properties of the primary cosmic ray flux and vary with altitude. It is noted that cosmic rays contribute to the radiation exposure of the population. For example, secondary neutrons with energies larger than about 100 keV are responsible for about half of the effective dose from cosmic radiation to aircrew and passengers at typical flight altitudes (Chen et al., 2008, 2010).

Therefore, various efforts have been made in the past to compute the radiation field in the atmosphere and measure the energy spectra of secondary neutrons from cosmic radiation at ground level (e.g. Schraube et al., 1997; 1999; Roesler et al., 1998; 2002; Heinrich et al., 1999). For this purpose, major efforts have also been made at the Helmholtz Zentrum München (HMGU) by developing an Extended Range Bonner Sphere Spectrometer (ERBSS) (Schraube et al., 1999; Mares et al., 1998), which is based on the initial standard BSS (Bramblett et al., 1960) but includes additional shells of lead in two polyethylene spheres. This allows accurate quantification of the neutron energy spectra in such high-energy fields. Since 2005, such ERBSSs have continuously monitored the neutrons from secondary cosmic radiation at the Environmental Research Station "Schneefernerhaus" at the Zugspitze mountain,

* Corresponding author.
E-mail address: tbrall@gmx.de (T. Brall).

https://doi.org/10.1016/j.radmeas.2021.106592
Received 19 November 2020; Received in revised form 29 April 2021; Accepted 3 May 2021
Available online 13 May 2021

Germany, and at the Koldewey Station of the Alfred-Wegener-Institute (AWI) in Ny-Ålesund, Spitsbergen, at sea level (Leuthold et al., 2007; Rühm et al., 2009).

Typically, an assessment of the neutron energy spectra in the atmosphere is done using Monte Carlo (MC) radiation transport codes. The present study uses the MC toolkit Geant4 (Version 10.1. patch 2) including treatment of thermal scattering as recommended (Agostinelli et al., 2003; Geant4 Collaboration, 2014). Recently it has been demonstrated that the response functions for a complete set of spheres used for an ERBSS are different when calculated with the Geant4 Bertini and Binary Intra Nuclear Cascade (INC) models (Rühm et al., 2014). These high-energy INC models must be used above 20 MeV, because evaluated cross section tables describing the interaction of relevant particles such as protons and neutrons for those energies with nuclei in the environment were not implemented in the Geant4 physics lists used in the present study. The differences in response functions mentioned above resulted in differences in unfolded neutron energy spectra measured with such an ERBSS at the Zugspitze mountain, Germany (Pioch et al., 2010). Along these lines, differences in response functions for selected Bonner spheres have also been obtained for different INC models when calculated with MC codes other than Geant4 (for example, MCNP (Briesmeister 1993), MCNPX (MCNPX 2008), PHITS (Niita et al., 2010, MARS (Mokhov 1995), FLUKA (Ferrari et al., 2005)) for neutron energies above 10 MeV (Rühm et al., 2014).

Benchmarking simulated response functions of Bonner spheres in quasi-mono-energetic neutron fields with neutron energies up to about 400 MeV did not allow for a conclusive answer as to which of the INC models used in Geant4 is preferable, due to the experimental uncertainties involved (Mares et al., 2013).

More recently, systematic dosimetric and spectrometric measurements and Geant4 simulations were performed scoring secondary neutrons produced at the CERN-EU high-energy Reference Field in Geneva, Switzerland (Wielunski et al., 2018; Brall et al., 2020). Specifically, for the spectrometric measurements an ERBSS was used at various locations outside the concrete and iron shielding of the CERF facility, and the resulting neutron energy spectra were compared with those simulated with Geant4 using the Binary and Bertini INC models (Brall et al., 2020). These authors stated that "both, in terms of total neutron fluence and neutron ambient dose equivalent, the results obtained with Geant4 using the Bertini physics list were somewhat closer to the measurements …. ". The overall conclusion of the study was, however, that "… no clear favorite of the two tested physics lists (Bertini or Binary), for the neutron field calculation at CERF, could be identified", because there was "no major difference between the Geant4 simulations and the ERBSS measurements performed" (Brall et al., 2020).

The prime aim of the present study was to validate the MC-simulated neutron spectra with experimental data and concurrently test the above conclusion. For this purpose, neutron energy spectra measured with an ERBSS at the "Umwelt-Forschungsstation Schneefernerhaus" (UFS) on the Zugspitze mountain, Germany, and at the Sphinx astronomical observatory on the Jungfraujoch, Switzerland (Mares et al., 2020), were compared with those obtained by dedicated simulations of secondary neutrons of cosmic radiation produced in the atmosphere using Geant4 with different INC models.

2. Materials and Methods

2.1. Measurement locations

The energy spectra of secondary cosmic ray neutrons used in this study had been deduced from ERBSS measurements at two different locations. The first neutron energy spectrum was measured at the environmental research station "Schneefernerhaus" (UFS) Zugspitze, Germany, in March 2018. This station is located at the south slope about 300 m below the Zugspitze summit at an altitude of 2650 m a.s.l. For this purpose, a stationary ERBSS was located in a measurement shed (3 × 7 m^2) on the terrace at the 5^{t}h floor of the station. The wooden shed has a steep roof covered by aluminium roof panels to avoid snow accumulation above the detectors mounted inside the shed (see Fig. 1). The second neutron energy spectrum was measured at the High-Altitude Research Station Jungfraujoch, Switzerland, in September 2018, using a mobile ERBSS. During this campaign the neutron energy spectrum was measured under the astronomical cupola on the upper floor of the Sphinx building at 3585 m a.s.l.. The building is located on top of the Sphinx rock. Its astronomical cupola has a diameter of 580 cm, a height of 420 cm, and is covered by a roof made of aluminium (see Fig. 2).

2.2. Monte Carlo simulations

The simulations in this work were done with the Monte Carlo (MC) Toolkit Geant4 (Agostinelli, S., 2003.) (Version 10.1. patch 2), calculated on a computer cluster parallelized with the Geant4 implementation of the Message Passing Interface (MPI) (https://www.mpi-forum.org/). The simulations were made for three different physics lists– "QGSP_BERT_HP", "QGSP_BIC_HP", and "Shielding" (Geant4 Collaboration, 2017), which are all reference physics lists of the Geant4 toolkit. The "QGSP_BERT_HP" and "QGSP_BIC_HP" physics lists both use the high precision neutron model (HP) for neutrons below 20 MeV, which is based on the G4NDL neutron cross section library. The main difference between these physics lists is the hadronic inelastic model used for neutrons and protons at energies up to 9.9 GeV: "QGSP_BIC_HP" uses the Binary INC model while "QGSP_BERT_HP" uses the Bertini INC model. The "Shielding" physics list represents an advancement of, but is close to the "FTFP BERT HP" physics list (which is the default physics list in Geant4 version used in the present work), includes the JENDL neutron cross section library, and is recommended for simulation of situations with significant shielding. More details about these physics lists are given in the Geant4 Guide for Physics Lists (Geant4 Collaboration, 2017).

The simulations involved a two-step process. In the first step, particles from a primary cosmic ray source at 100 km a.s.l. (see chapter 2.1.1) were transported (about 1.3 million protons and about 300,000 alpha particles) through an atmospheric cylinder with a radius of 3000 km (see chapter 2.1.2) down to a pre-defined altitude (3 km a.s.l. for the UFS geometry, and 3.6 km for the Sphinx geometry). Particles passing the bottom of the disc (the "coupling surface") were scored with respect to momentum (for example, number of scored neutrons: about 350,000 at 3 km and about 500,000 at 3.6 km). In the second step, a simulation was started with the particle momenta scored in the first step (i.e., at 3 km or 3.6 km a.s.l) (typically, the number of started particles was chosen such that the statistical uncertainties in the detector reading was below 5% for total neutron fluence), including the full geometry with the atmosphere from the ground up to an altitude of 100 km, but with a smaller diameter of 40 km. The ground was either modelled as a slanted surface (to model the UFS environment) or as a pyramid (to model the Sphinx environment) (see chapter 2.1.3). Any biasing techniques other than the two-step simulation were not used.

This two-step approach allowed simulation of a much smaller volume for step 2 as compared to that used for step 1, without compromising the neutron energy spectra simulated at the detector locations from boundary effects. By keeping the source closer to the detector volume in step two, CPU time was reduced. The approach was particularly useful for an accompanying study where detailed sensitivity analyses were done to study the influence of environmental parameters such as snow height and soil moisture on the neutron energy spectra (for such studies the particles scored in step 1 at the boundary surface were used, and only step-2 simulations had to be carried out).

2.2.1. Primary cosmic ray spectrum

In the simulations the source term consisted of primary protons and alpha particles (heavier particles were neglected) from cosmic radiation hitting the top of the atmosphere at an altitude of 100 km. The source

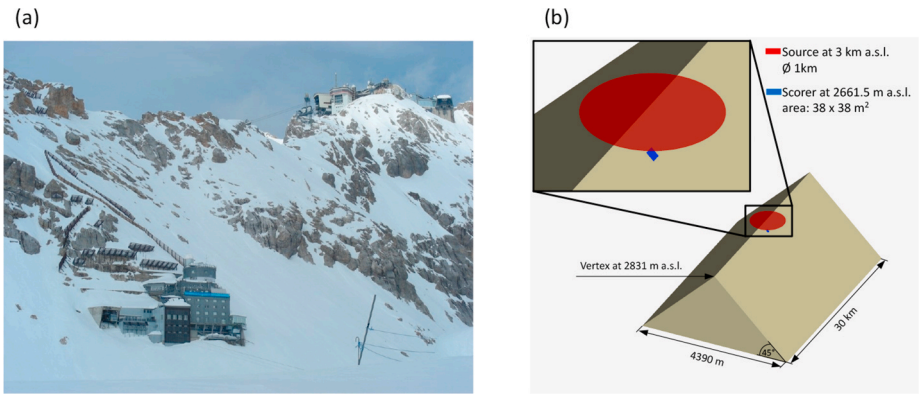

Fig. 1. a) Picture of the UFS Research Station at the Zugspitze (Photo: V. Mares). b) geometry as implemented in the Geant4 simulations.

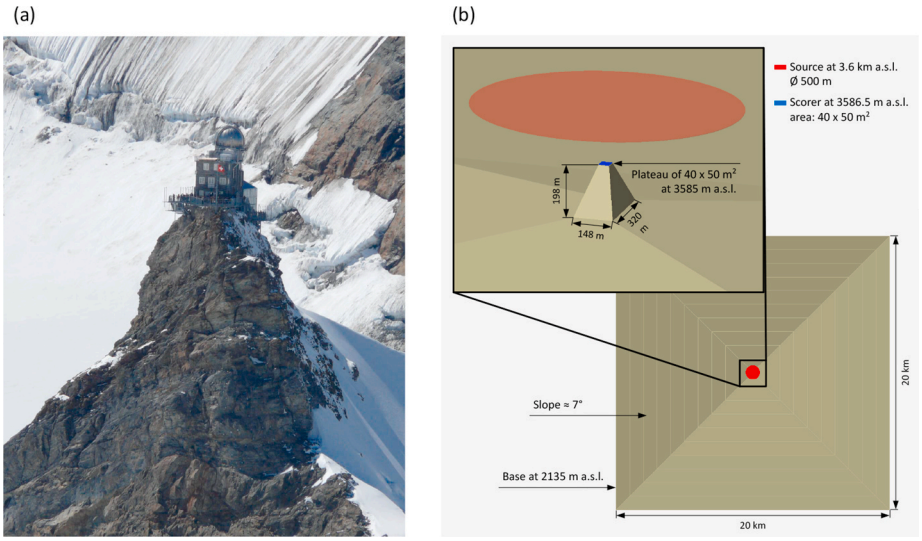

Fig. 2. a) Picture of the Sphinx Cupola at Jungfraujoch (Photo: V. Mares). b) Geometry as implemented in the Geant4 simulations.

was implemented as a small circular plane with a diameter of 10 cm (i.e., compared to the size of the total simulated volume it can be considered as a point source), placed at the central axis of the atmospheric cylinder. For the angular distribution through the surface area of the plane source a cosine law distribution was used (Lambert's cosine law). The cosmic radiation spectrum for protons, J_{LIS}, implemented in the simulation was based on the local interstellar (LIS) spectrum outside the heliosphere developed by (Burger et al., 2000; Usoskin et al., 2005) (Eq. (1))

$$J_{LIS} = \frac{1.9 \cdot 10^4 \, P(T)^{-2.78}}{1 + 0.4866 \, P(T)^{-2.51}} \quad (1)$$

$$\text{with} \quad P(T) = \sqrt{T(T + 2T_r)}$$

Where $P(T)/c$ is the momentum of a particle with rest mass energy T_r (e.g., 938 MeV for protons). T is the kinetic energy per nucleon expressed in GeV/nucleon while J_{LIS} is expressed in particles per (m^2 sr s GeV/nucleon).

The differential intensity for helium can be obtained by weighting Eq. (1) with the proton to helium ratio in particle numbers of 0.05 (Usoskin et al., 2005). Modulation of the LIS spectrum within the solar system is described by the so-called modulation function $\Phi(t)$ (Eq. (2)) which describes the mean energy loss a cosmic ray nucleus experiences in the solar wind while traveling from the termination shock of the heliosphere to the Earth as function of time, t.

$$\Phi(t) = \frac{Ze}{A} \varphi(t) \quad (2)$$

Where e denotes the elementary charge, Z the charge number, A the mass number, and $\varphi(t)$ in the unit MV is the so-called modulation parameter or modulation potential which was taken from Usoskin et al., (2005).

Consequently, the differential intensity J_i of cosmic ray nuclei of type i close to the Earth at a distance from the Sun of 1 astronomical unit (1 AU, corresponding to about 1.5×10^8 km) is given by Eq. (3):

$$J_i(T, \varphi) = J_{LIS,\,i}(T + \Phi) \frac{(T)(T + 2T_r)}{(T + \Phi)(T + \Phi + 2T_r)} \quad (3)$$

To approximate the conditions of solar minimum in September 2018, a modulation potential of 420 MV was used for the simulations.

In order to take account of the shielding of primary cosmic radiation by the magnetic field of the Earth, a cutoff rigidity of 4.2 and 4.5 GV was used for the Zugspitze and Jungfraujoch regions. This corresponds to cutoff energies of 3.37 GeV/nuc for protons and 1.37 GeV/nuc for alpha particles at Zugspitze, and 3.66 GeV/nuc for protons and 1.50 GeV/nuc for alpha particles at Jungfraujoch.

In the simulations, protons with energies of up to 1 TeV and alpha particles with energies up to 100 GeV/nuc were implemented. The corresponding energy spectra are shown in Fig. 3.

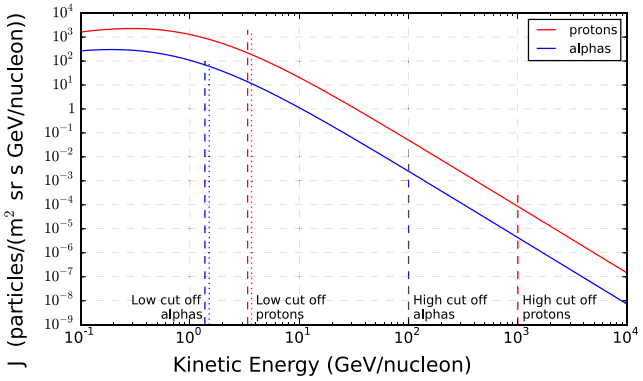

Fig. 3. Primary Cosmic Ray Spectra of protons and alpha particles as calculated with Eq. (3). For solar minimum conditions with a modulation potential of 420 MV; vertical lines – energy cut off for UFS (dashed) and Jungfraujoch (dotted); note that different low-energy cut offs for UFS and Jungfraujoch are due to different geomagnetic fields.

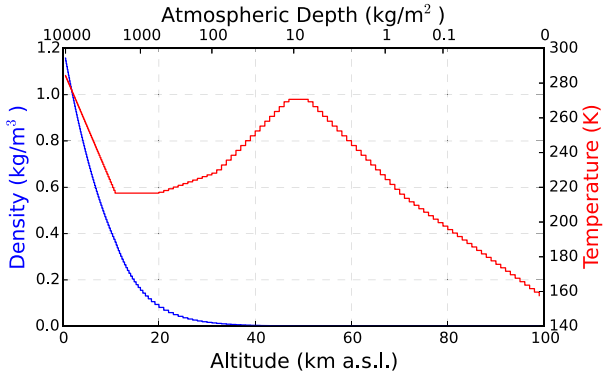

Fig. 4. Density (blue curve) and temperature vs. altitude/atmospheric depth profiles used in the Geant4 simulations, according to the U.S. Standard Atmosphere 1976 (COESA 1976). (For interpretation of the references to colour in this figure legend, the reader is referred to the Web version of this article.)

2.2.2. Model of earth atmosphere

For the MC simulations of the GCR interactions in the atmosphere, the atmosphere was constructed as a cylinder with a diameter of 6000 km and a height of 100 km (from sea level to 100 km a.s.l.). The height of 100 km was chosen to cover most of the atmosphere in terms of atmospheric depth (about 2 mg/m^2 at 100 km of about 10,300 kg/m^2 at sea level). The diameter was chosen to ensure that loss of particles from secondary cosmic rays due boundary effects is negligible. To reproduce the temperature and density profile, the atmospheric cylinder was divided into layers equidistant in atmospheric depth up to an altitude of 20 km, with a thickness of about 10 g/cm^2 (corresponding to 100 kg/m^2). At altitudes higher than 20 km the thickness of these layers was set to 1 km. The parameters of the Earth's atmosphere and its elemental composition (Table 1) were implemented according to the US Standard Atmosphere 1976 (COESA 1976). The corresponding density and temperature profiles against the altitude are shown in Fig. 4. It is noted that variations in parameters such as water vapor in the atmosphere or humidity in the environment (e.g., soil moisture) were considered to be out-of-scope of the present study. Analyses of the influence of such parameters on the neutron spectrum from secondary cosmic rays at ground level have been done in a companion study (Brall et al., 2021).

With this geometry of the atmosphere, the momenta of secondary particles (such as protons and neutrons, but also alpha particles, deuterons, electrons and positrons, photons, muons, pions, kaons, etc.) were scored at the coupling surface at an altitude of 3 km for the Zugspitze mountain, and at an altitude of 3.6 km for Jungfraujoch. At this stage, out of about 1.6 million primary particles used as a source in step 1, about 350,000 at 3 km and about 500,000 at 3.6 km secondary neutrons were scored. The scored momenta (including momentum direction) of all particles were then directly used for the definition of the source particles in the second step. The simulations in the second step included an atmospheric volume with a height of 100 km and a diameter of 40 km, and soil (see chapter 2.1.3). The geometric dimensions were again chosen to ensure that loss of particles from secondary cosmic rays due to boundary effects is negligible, to allow the implementation of mountain topology, and also to reduce the time needed for the computer simulations. In this step, particle momenta scored at the coupling surface in the first step were used as a primary source (Fig. 5, right panel).

Table 1
Elemental composition of air expressed as mass fractions used in the Geant4 simulations corresponding to the U.S. Standard Atmosphere 1976 (COESA 1976).

Element	Mass Fraction
N	0.755
O	0.232
Ar	0.0128
C	0.000124

2.2.3. Ground geometry

In order to account for albedo neutrons, different soil geometries were implemented.

- Zugspitze mountain

The geometry of the Zugspitze mountain (Fig. 1 a) was implemented as a volume with a width of 4390 m; a length of 30 km; a height of 2195 m; a slant angle of 45° (Fig. 1 b) as estimated for the slope at the UFS position based on GDEM (Global Digital Elevation Map) V3 from the ASTER (Advanced Spaceborne Thermal Emission and Reflection Radiometer) instrument onboard the Terra satellite (see https://asterweb.jpl.nasa.gov/gdem.asp; downloaded from https://search.earthdata.nasa.gov/search/on 23. July 2019; ASTER GDEM is a product of METI and NASA). On one of the slant surfaces of the volume the UFS was located, where the ERBSS measurements were performed (see chapter 2.2). The vertex was assumed at 2831 m a.s.l. which corresponds to the height of the mountain ridge above the UFS (see Fig. 1 a), and a scorer of the size 38 × 38 m^2 was defined at an altitude of 2661.5 m a.s.l. which corresponds to the altitude of the UFS (1.5 m above ground). The material used for the soil was limestone ($CaCO_3$) with a density of 2.8 g/cm^3. Simulations were done assuming a snow cover of 50 cm on the ground equivalent to a water layer of 12.5 cm (as the measurements were performed in March 2018, i.e., during conditions typical for winter season).

- Jungfraujoch

The Sphinx cupola at the Jungfraujoch, where additional ERBSS measurements were carried out (chapter 2.3), is on the top of the Sphinx building at 3585 m a.s.l. (including the height of the measurement location of the ERBSS above the summit of the Sphinx rock). Consequently, the geometry was modelled as a volume with a height of 198 m; a width of 148 m; and a length of 320 m, flattened at the top, and again made of limestone with a density of 2.8 g/cm^3. A scorer of 40 × 50 m^2 located 1.5 m above ground of the flattened plateau served as detector. Thus, the real geometry including the summit and the Sphinx building (Fig. 2 b) was simplified and modelled as being completely made of limestone (Fig. 2 b). This simplification was necessary, due to the lack of detailed information of construction geometry and the elemental composition of the construction materials of the Sphinx cupola.

Because the measurements at the Jungfraujoch were performed in

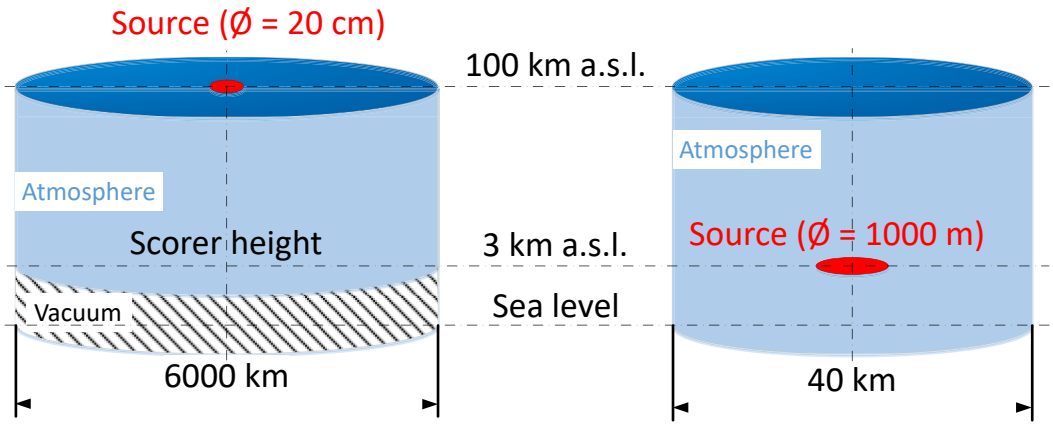

Fig. 5. Illustration of atmospheric model as implemented in Geant4. Left panel: geometry for step 1 of the simulations; Right panel: geometry for step 2 of the simulations. Figures are not drawn to scale. For details see text.

September 2018 during conditions typical for summer times (i.e., not much snow (Mares et al., 2020)), no snow cover was assumed on the ground. However, for comparison, additional simulations were performed with the ground covered by a snow layer of 50 cm (corresponding to a snow-water-equivalent (SWE) layer of 12.5 cm assuming a snow density of 250 kg/m^3 which had been measured in the vicinity of the UFS (Hürkamp et al., 2019). (It should be noted that detailed information on the height of the snow cover in the close vicinity of the measurement positions was not available.).

2.3. Bonner sphere measurements

Complementary to the MC simulations described above, the energy spectra of neutrons from secondary cosmic radiation were deduced from ERBSS measurements both at the UFS on the Zugspitze mountain, Germany, and in the Sphinx astronomical observatory on the Jungfraujoch, Switzerland. Since 2005, an ERBSS has been used to continuously monitor the neutron energy spectra at the Zugspitze mountain. A similar but mobile ERBSS was used for the measurements at the Jungfraujoch, Switzerland. Details on these ERBSS spectrometers are given in (Mares et al. 1998, 2020; Leuthold et al., 2007; Pioch et al., 2010; Brall et al., 2020). Briefly, both ERBSS systems consist of a set of polyethylene spheres with different diameters, with ^{3}He proportional counters in their centers. These counters detect neutrons that impinged the spheres at various energies and were moderated and thermalized by the spheres on their way to the counters. One proportional counter without any polyethylene casing was used in each spectrometer to detect thermal neutrons in the environment. The neutron-induced nuclear reactions ((n,2n) and (n,3n)) in lead included in two 9-inch spheres multiply the number of secondary neutrons and increase significantly the counting rate for high-energy neutrons (E > 20 MeV) (Mares et al., 1998). These modified spheres were used both for the measurements at Zugspitze and Jungfraujoch. Additionally, 13 standard polyethylene Bonner spheres were used for the Zugspitze measurements, while 15 standard polyethylene Bonner spheres were used for the Jungfraujoch measurements.

Due to the different sizes of these polyethylene spheres, the ERBSS allows neutron spectrometry in a wide range of energies from meV up to GeV. This is done by applying an unfolding procedure which requires an initial guess neutron spectrum, a response matrix (which describes the response of each individual proportional counter including casing per incoming neutrons as a function of neutron energy), and the count rates obtained by the individual proportional counters of the ERBSS. For details see Mares et al., 1998.

For neutrons from secondary cosmic rays measured at ground level, uncertainties in total measured neutron fluence related to the choice of the guess spectrum were shown to be less than 1% (Simmer et al., 2010), those related to the choice of the unfolding code used were shown to be less than 4% (Barros et al., 2014), and those related to the choice of response matrix were shown to be less than 5% (Pioch et al., 2010). Consequently, the total uncertainty in measured total neutron fluence is about 7% when error propagation is used. This is consistent with an overall uncertainty of about 10% in total neutron fluence that was estimated in Brall et al., 2020 for the neutron spectrum measured at the CERF facility, which was close to the neutron spectra measured in the present study (Brall et al., 2020).

For the purpose of the present paper, neutron energy spectra measured in March 2018 at the UFS (i.e., when there was a significant snow cover in the close environment of the ERBSS), and measured in September 2018 at the Sphinx laboratory (i.e., during a period of minimum snow cover), were used. The spectra obtained at the Jungfraujoch were already described in an earlier paper (Mares et al., 2020).

Finally it is noted that the MC codes and high-energy nuclear models used in the present paper to calculate the response matrix of the ERBSS (i.e., a combination of MCNP and LAHET (Mares et al., 1991; 1998) were different from those used here to calculate the environmental spectra from secondary cosmic rays (i.e., the Geant4 code).

3. Results and discussion

3.1. UFS laboratory at Zugspitze

Fig. 6 shows the neutron energy spectra calculated for and measured at the UFS (the fine structure seen in the spectrum (in the region between 400 keV and about 10 MeV) is mainly due to resonances in the interaction cross sections for nitrogen and oxygen in air). The simulated spectra were calculated with the "QGSP_BERT_HP", "QGSP_BIC_HP", and "Shielding" physics lists provided by Geant4. For the unfolding process of the measured ERBSS count rates the three simulated neutron energy spectra were each used as guess spectrum. Fig. 6 demonstrates a reasonable agreement between measured and simulated neutron energy spectra. All simulated and measured spectra reveal the characteristic four energy regions – thermal region, epithermal region, evaporation region, and cascade region. The right panel of Fig. 6 shows the corresponding integrated neutron fluences for these four energy regions.

3.1.1. Comparison of simulation and measurements

A reasonable qualitative agreement between simulations and measurements can be observed in Fig. 6. It is noted, however, that this agreement is basically due to the height of the snow cover chosen for the simulations (12.5 cm snow water equivalent). Clearly, the agreement might have been worse if other snow heights were chosen. Consequently, a systematic study on the influence of snow and other sources of hydrogen in the environment such as soil humidity close to the ERBSS is needed before a more meaningful quantitative comparison between

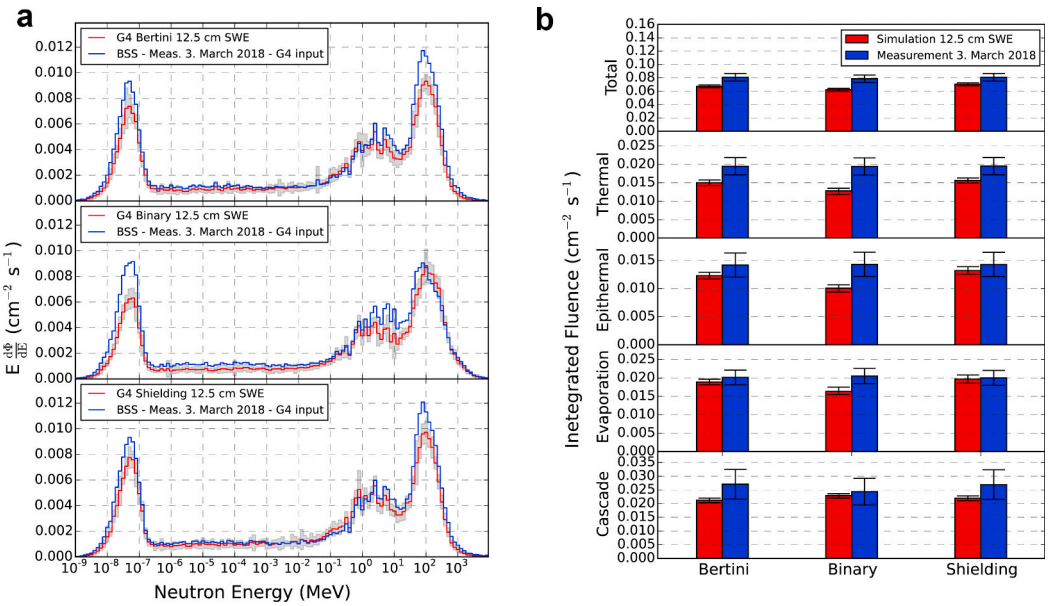

Fig. 6. Left: Red lines - Neutron energy spectra at the UFS (Zugspitze) simulated with three physics lists ("QGSP_BERT_HP", "QGSP_BIC_HP" and "Shielding") and assuming a snow cover of 12.5 cm SWE; Blue lines - unfolded measured ERBSS spectra with the corresponding simulated neutron energy spectra used as guess spectra for the unfolding. Grey shadow – bin-per-bin standard deviation; Right: Corresponding total fluence and fluence in the four energy regions (thermal: E < 0.4 eV; epithermal: 0.4 eV ≤ E < 100 keV; evaporation: 100 keV ≤ E < 20 MeV and cascade: E ≥ 20 MeV); blue bars – based on measured neutron energy spectra at UFS (Zugspitze); red bars- based on simulated neutron energy spectra. Measurements were performed on 3 March 2018; error bars: standard deviation for the simulations (red bars), and experimental uncertainties (blue bars). (For interpretation of the references to colour in this figure legend, the reader is referred to the Web version of this article.)

measured and simulated neutron energy spectra can be made.

It is interesting, however, that the agreement between simulations and measurements for the cascade region where the neutron energy spectra are generally not much influenced by the water content of the environment (Rühm et al., 2012) appears somewhat better for the "QGSP_BIC_HP" physics list (6% lower than measured) than for the "QGSP_BERT_HP" (22% lower than measured) and "Shielding" physics lists (19% lower than measured). An agreement between measurement and simulation at the cascade region of about 10%–20% is considered reasonable, given the uncertainties involved in the simulations (e.g., nuclear models, simplified geometry of the atmosphere, the mountain, and the local environment) and the measurements (see also section "2. Materials and Methods" where uncertainties in simulations and measurements are discussed). Overall, the agreement between simulated and measured fluences in the cascade region is remarkable.

3.1.2. Comparison of physics lists

Overall, differences between the three simulated spectra calculated with the three different physics lists are remarkably small, especially for total cascade neutrons (0.0212 1/cm^{2}s for "QGSP_BERT_HP", 0.0229 1/cm^{2}s for "QGSP_BIC_HP", 0.0219 1/cm^{2}s for "Shielding") and typically within less than ± 5%.

For the evaporation neutrons the corresponding results are (0.0189 1/cm^{2}s for "QGSP_BERT_HP", 0.0164 1/cm^{2}s for "QGSP_BIC_HP", 0.0197 1/cm^{2}s for "Shielding") and typically within about ±10%.

For the epithermal neutrons the corresponding results are (0.0123 1/cm^{2}s for "QGSP_BERT_HP", 0.0101 1/cm^{2}s for "QGSP_BIC_HP", 0.0132 1/cm^{2}s for "Shielding") and typically within about ±15%.

Finally, for the thermal neutrons the corresponding results are (0.015 1/cm^{2}s for "QGSP_BERT_HP", 0.0128 1/cm^{2}s for "QGSP_BIC_HP", 0.0156 1/cm^{2}s for "Shielding") and typically within about ±10%.

These results demonstrate that there are no major differences between the results obtained with the three physics lists.

3.1.3. Comparison with FLUKA

In (Roesler et al., 2002) similar calculations were carried out with the FLUKA code. In those calculations, a layer of 50 cm concrete (to simulate the influence of the UFS building on the measurements) at an altitude of 2660 m a.s.l. was assumed, with a snow layer of 10 cm (corresponding to 3 cm SWE), and a scorer 1 m above ground was implemented. For an experimental validation they used a similar ERBSS as was used in the present study, but with 12 measurement channels (bare detector, 2.5, 3, 4, 5, 6, 7, 9, 10, 12, 15 inch, and a 9 inch sphere including a lead shell). These measurements were carried out in March 1997, at the time of solar minimum. In their experiment, the ERBSS was housed in aluminium boxes. Therefore, in the simulations they placed two aluminium layers (thickness: 2 mm) 30 cm above and below the FLUKA scorer. A total water column of 7.5 mm was assumed in air, to take into account water vapor in the atmosphere. In their paper, Roesler et al. folded the calculated FLUKA spectra with the ERBSS response functions to calculate count rates of the ERBSS detectors. Consequently, in the present paper the same approach was followed and the calculated Geant4 spectra were folded with the corresponding ERBSS response functions. The resulting count rates were then compared to those given by Roesler and co-workers. It turned out that, typically, the Geant4 count rates obtained in the present study were lower by about a factor of 2.5, when the G4_BIC_HP physics list was used. This might be due to the following reasons: a) in the FLUKA calculations the mountain geometry and its shielding effect was not included, which would result in a decrease of count rates between about 20% and 50%, depending on neutron energy region and snow conditions (Brall et al., 2021), and b) Roesler and co-workers assumed an SWE layer of 3 cm in their simulations, while the Geant4 simulations described in the present study assumed an SWE layer of 12.5 cm; it will be shown in a complementary paper that such a difference in SWE height leads to an increase in neutron fluence by about a factor of 2, again depending on neutron energy range. Details are given in (Brall et al., 2021).

3.2. Sphinx Observatory at Jungfraujoch

Fig. 7 shows the corresponding neutron energy spectra calculated for and measured at the Sphinx cupola on the Jungfraujoch (as for Fig. 6: Left: Red lines - Neutron energy spectra at the UFS (Zugspitze) simulated with three physics lists ("QGSP_BERT_HP", "QGSP_BIC_HP" and "Shielding") and assuming a snow cover of 12.5 cm SWE; Blue lines -

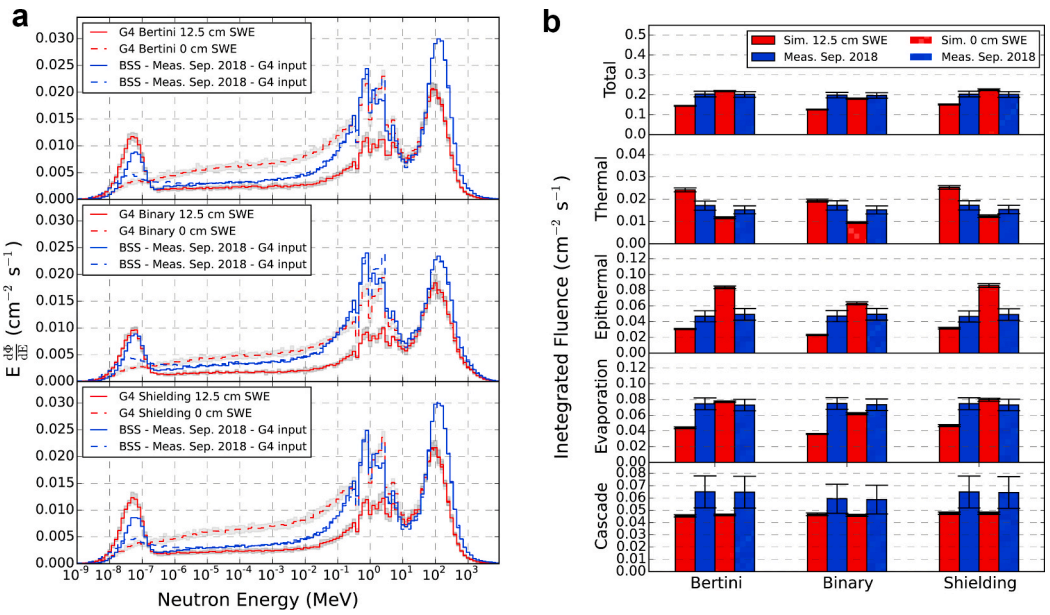

Fig. 7. Left: Red lines - Neutron energy spectra at the Sphinx cupola (Jungfraujoch) simulated with three physics lists ("QGSP_BERT_HP", "QGSP_BIC_HP" and "Shielding") and assuming a snow cover of 0 cm (dashed lines) and 12.5 cm SWE (solid lines); Blue lines - unfolded measured ERBSS spectra with the corresponding simulated neutron energy spectra (with (solid lines) or without (dashed lines) snow) used as guess spectra for the unfolding. Grey shadow – bin-per-bin standard deviation. Right: Corresponding total fluence and fluence in the four energy regions (thermal: E < 0.4 eV; epithermal: 0.4 eV ≤ E < 100 keV; evaporation: 100 keV ≤ E < 20 MeV and cascade: E ≥ 20 MeV); blue bars – based on measured neutron energy spectra at the Sphinx cupola (Jungfraujoch); red bars-based on simulated neutron energy spectra. With 12.5 cm SWE (plain bars) and 0 cm SWE (hatched bars). Measurements were performed in September 2018. Error bars: standard deviation for the simulations (red bars), and experimental uncertainties (blue bars) The measured neutron spectra shown here are very similar to those given in Mares et al., (2020) for June 2016, during similar environmental conditions. (For interpretation of the references to colour in this figure legend, the reader is referred to the Web version of this article.)

unfolded measured ERBSS spectra with the corresponding simulated neutron energy spectra used as guess spectra for the unfolding. Grey shadow – bin-per-bin standard deviation; Right: Corresponding total fluence and fluence in the four energy regions (thermal: E < 0.4 eV; epithermal: 0.4 eV ≤ E < 100 keV; evaporation: 100 keV ≤ E < 20 MeV and cascade: E ≥ 20 MeV); blue bars – based on measured neutron energy spectra at UFS (Zugspitze); red bars-based on simulated neutron energy spectra. Measurements were performed on 3 March 2018; error bars: standard deviation for the simulations (red bars), and experimental uncertainties (blue bars)., the fine structure seen in the spectrum (in the region between 400 keV and about 10 MeV) is mainly due to resonances in the interaction cross sections for nitrogen and oxygen in air). As for the UFS at the Zugspitze (Fig. 6) the simulated spectra used the "QGSP_BERT_HP", "QGSP_BIC_HP" and "Shielding" physics lists. In the case of the Sphinx cupola on the Jungfraujoch the simulations were performed without snow cover and with a snow cover with a thickness corresponding to 12.5 cm snow water equivalent. As for Fig. 6, the measured ERBSS count rates were done using the calculated spectra as guess spectra in the unfolding process.

3.2.1. *Comparison of simulation and measurements*

Again, reasonable qualitative agreement between simulations and measurements can be observed in Fig. 7. It is noted, however, that this agreement is somewhat worse when a height of the snow cover of 12.5 cm snow water equivalent was chosen for the simulations (note that the snow water equivalent of 12.5 cm was chosen to allow comparison with the simulations performed for the UFS (Fig. 6); we also note that in reality such a snow height is unlikely around the Sphinx Observatory, even at winter times (Mares et al., 2020), probably because of the steep slope of the rock on which the Observatory is located (Fig. 2a)). In contrast, for the case when no additional snow cover was considered, the shape of the simulated neutron energy spectra changed significantly, in particular at neutron energies below 20 MeV in the evaporation, epithermal and thermal energy regions. As already discussed above for the UFS case, a systematic study on the influence of snow and other sources of hydrogen in the environment close to the ERBSS is needed before a more meaningful quantitative comparison between measured and simulated neutron energy spectra can be made.

As has already been observed for the UFS case, the agreement between simulations and measurements for the cascade region where the neutron energy spectra are generally not much influenced by the water content of the environment (Rühm et al., 2012) is reasonable: For the "QGSP_BIC_HP" physics list the simulated fluence is about 22% lower, for the "QGSP_BERT_HP" physics list it is 29% lower than measured, and for the "Shielding" physics lists it is about 26% lower (see also section "2. Materials and Methods" where uncertainties in simulations and measurements are discussed) (see right panel of Fig. 7).

3.2.2. *Comparison of physics lists*

Overall, differences between the three simulated spectra calculated with the three different physics lists are rather small, especially for total cascade neutrons (0.046 1/cm^{2}s for "QGSP_BERT_HP", 0.046 1/cm^{2}s for "QGSP_BIC_HP", 0.048 1/cm^{2}s for "Shielding"), i.e., typically within less than ± 5%.

For the evaporation neutrons the corresponding results are (0.077 1/cm^{2}s for "QGSP_BERT_HP", 0.062 1/cm^{2}s for "QGSP_BIC_HP", 0.080 1/cm^{2}s for "Shielding"), i.e., typically within about ±15%.

For the epithermal neutrons the corresponding results are (0.084 1/cm^{2}s for "QGSP_BERT_HP", 0.063 1/cm^{2}s for "QGSP_BIC_HP", 0.086 1/cm^{2}s for "Shielding"), i.e., typically within about ±20%.

Finally, for the thermal neutrons the corresponding results are (0.022 1/cm^{2}s for "QGSP_BERT_HP", 0.018 1/cm^{2}s for "QGSP_BIC_HP", 0.023 1/cm^{2}s for "Shielding"), i.e., typically within about ±15%.

These results demonstrate again, as was already seen for the neutron energy spectra simulated for the UFS at the Zugspitze mountain, that there are no major differences between the results obtained with the three physics lists.

4. Conclusions

In the study described here, measured and simulated energy spectra of secondary neutrons from cosmic radiation at ground level were systematically compared. For the measurements, a stationary ERBSS system was used that was located at the UFS on the Zugspitze mountain,

Germany, at an altitude of 2650 m a.s.l.. A second mobile ERBSS system was used to measure at an altitude of 3585 m a.s.l. below the cupola of the astronomical observatory at the top of Sphinx building on the Jungfraujoch, Switzerland.

Radiation transport calculations were performed assuming a state-of-the-art energy spectrum (protons and alpha particles) of primary cosmic radiation impinging on top of the atmosphere. Particle transport through the atmosphere and in soil were performed using the Geant4 Monte Carlo toolkit including three different physics lists - "QGSP_BERT_HP", "QGSP_BIC_HP" and "Shielding". These physics lists are important in particular at high energies above 20 MeV where experimental data on interaction cross sections are scarce and nuclear models must be used to calculate these cross sections. For low-energy neutrons, additional extended physics lists are available in Geant4 such as the Shielding-LEND physics list. This physics list was not used in the present study but should be investigated in the future.

For both measurement locations, simulated and measured neutron energy spectra agreed remarkably well, in particular at high energies above 20 MeV. However, due to the unknown hydrogen content (snow cover and soil water) in the close environment of the ERBSS systems, a final conclusion on the agreement between simulations and measurements cannot be made at lower neutron energies, in particular in the thermal and epithermal energy region where environmental hydrogen plays a crucial role in moderating and absorbing neutrons. Currently, a systematic study is under way investigating the influence of environmental hydrogen on the shape of the energy spectrum of secondary neutrons from cosmic radiation at ground level, with particular emphasis on low-energy neutrons (Brall et al., 2021).

The present study demonstrated that for both locations, differences in simulated neutron energy spectra obtained with the three different Geant4 physics lists were small (between ±5% and ±20%, depending on the energy region of the neutron spectrum, and location). This confirmed results reported recently for the CERF facility at CERN (Brall et al., 2020) where secondary neutron spectra outside the CERF shielding were similar to those measured in the present study for secondary neutrons from cosmic radiation, and where differences were also small when different Geant4 physics lists were used in the simulations. It is concluded that the use of different physics lists is not of critical concern when MC simulations are performed in an effort to calculate radiation doses from cosmic radiation to aircrew.

Declaration of competing interest

The authors declare that they have no known competing financial interests or personal relationships that could have appeared to influence the work reported in this paper.

Acknowledgement

We would like to thank the staff of the UFS "Schneefernerhaus" for their long-term support in the ERBSS measurements, the staff of the High-Altitude Research Station Jungfraujoch, and the International Foundation High Altitude Research Stations Jungfraujoch and Gornergrat for free use of the infrastructure required for the measurements. This research received funding from the Bavarian State Ministry of the Environment and Consumer Protection, within the research project "Virtual Alpine Observatory" under contract number "71_1d-U8729-2013/193-5".

References

ASTER Global Digital Elevation Map. https://asterweb.jpl.nasa.gov/gdem.asp.
Agostinelli, S., 2003. Geant4 - a simulation toolkit. Nucl. Instrum. Methods Phys. Res., Sect. A 506, 250–303.
S. Barros, S., Mares, V., Bedogni, R., Reginatto, M., Esposito, A., Gonçalves, I.F., Vaz, P., Rühm, W., 2014. Comparison of unfolding codes for neutron spectrometry with Bonner spheres Radiat. Protect. Dosim. 161 (1–4), 46–52.
Brall, T., Dommert, M., Rühm, M., Trinkl, S., Wielunski, M., Mares, V., 2020. Monte Carlo simulation of the CERN-EU high energy Reference Field (CERF) facility. Radiat. Meas. 133, 106294.
Brall, T., Mares, V., Bütikofer, R., Rühm, W., 2021. Assessment of neutrons from secondary cosmic rays at mountain altitudes – Geant4 simulations of environmental parameters including soil moisture and snow cover. In preparation.
Bramblett, R.L., Ewing, R.I., Bonner, T.W., 1960. A new type of neutron spectrometer. Nucl. Instrum. Methods Phys. Res. 9, 1–12.
Briesmeister, J.F. (Ed.), 1993. MCNP - A General Monte Carlo N-Particle Transport Code, Version 4A. LA-12625-M. Los Alamos National Laboratory.
Burger, R., Potgieter, M., Heber, B., 2000. Rigidity dependence of cosmic ray proton latitudinal gradients measured by the Ulysses spacecraft: implications for the diffusion tensor. Journal of Geophysical Research (Space Physics) 105 (A12), 27447–27455.
Chen, J., Mares, V., 2008. Estimate of doses to the fetus during commercial flights. Health Phys. 95, 407–412.
Chen, J., Mares, V., 2010. Significant impact on effective doses received during commercial flights calculated using the new ICRP radiation weighting factors. Health Phys. 98, 74–76.
COESA, U.S. Standard Atmosphere, 1976. Technical report NOAA document S/T 76-1562, committee on extension to the standard atmosphere (COESA), national oceanic and atmospheric administration (NOAA), the national aeronautics and space administration (NASA), U.S. Air force, 1976.
Earthdata, Nasa. https://search.earthdata.nasa.gov/search/.
Ferrari, A., Sala, P., Fassò, A., Ranft, J., 2005. FLUKA: A Multi-Particle Transport Code. Geant4 Collaboration. CERN-2005-10, INFN/TC_05/11, SLAC-R-773, 2017.
Forum, M.P.I.. https://www.mpi-forum.org/.
Geant4 Collaboration, 2014. Geant4 User's Guide for Aplication Developers. Version: 10.1. http://geant4-userdoc.web.cern.ch/geant4-userdoc/UsersGuides/ForApplicationDeveloper/BackupVersions/V10.1/html/index.html.
Geant4 Collaboration, 2017. Guide for Physics Lists Release 10, vol. 4. http://geant4-userdoc.web.cern.ch/geant4-userdoc/UsersGuides/PhysicsListGuide/BackupVersions/V1.0.4/html/index.html.
Heinrich, W., Roesler, S., Schraube, H., 1999. Physics of cosmic radiation fields. Radiat. Protect. Dosim. 86 (4), 253–258.
Hürkamp, K., Zentner, N., Reckerth, A., Weishaupt, S., Wetzel, K.-F., Tschiersch, J., Stumpp, C., 2019. Spatial and temporal variability of snow isotopic composition on Mt. Zugspitze, Bavarian Alps, Germany. J. Hydrol. Hydromechanics 67, 49–58.
Leuthold, G., Mares, V., Rühm, W., Weitzenegger, E., Paretzke, H., 2007. Long-term measurements of cosmic ray neutrons by means of a Bonner spectrometer at mountain altitudes - first results. Radiat. Protect. Dosim. 126 (1–4), 506–511.
Mares, V., Schraube, H., 1998. High energy neutron spectrometry with Bonner spheres. In: Proceedings, the IRPA Regional Symposium on Radiation Protection in Neighbouring Countries of Central Europe. Czech Republic, Prague, pp. 543–547. September 1997.
Mares, V., Pioch, C., Rühm, W., Iwase, H., Iwamoto, Y., Hagiwara, M., Satoh, D., Yashima, H., Itoga, T., Sato, T., Nakane, Y., Nakashima, H., Sakamoto, Y., Matsumoto, T., Masuda, A., Harano, H., Nishiyama, J., Theis, C., Feldbaumer, E., Jaegerhofer, L., Tamii, A., Hatanaka, K., Nakamura, T., 2013. Neutron dosimetry in quasi-monoenergetic fields of 244 and 387 MeV. IEEE Trans. Nucl. Sci. 60, 299–304.
Mares, V., Brall, T., Bütikofer, R., Rühm, W., 2020. Influence of environmental parameters on secondary cosmic ray neutrons at high-altitude research stations at Jungfraujoch, Switzerland, and Zugspitze, Germany. Radiat. Phys. Chem. 168, 108557.
Mares, V., Schraube, G., Schraube, H., 1991. Calculated neutron response of a Bonner sphere spectrometer with 3He counter. Nucl. Instrum. Methods A 307, 398–412.
Mokhov, N.V., 1995. The Mars Code System User's Guide, vol. 628. Fermilab-FN.
Niita, K., Matsuda, N., Iwamoto, Y., Iwase, H., Sato, T., Nakashima, H., Sakamoto, Y., Sihver, L., 2010. PHITS: Particle and Heavy Ion Transport Code System. Japan Atomic Energy Agency. JAEA-Data/Code 2010-022, Version 2.23.
Pelowitz, D.B. (Ed.), 2008. MCNPX User's Manual Version 2.6.0, LA-CP-07-1473. Los Alamos National Laboratory. April.
Pioch, C., Mares, V., Rühm, W., 2010. Influence of Bonner sphere response functions above 20 MeV on unfolded neutron spectra and doses. Radiat. Meas. 45, 1263–1267.
Roesler, S., Heinrich, W., Schraube, H., 1998. Calculation of radiation fields in the atmosphere and comparison to experimental data. Radiat. Res. 149 (1), 87–97.
Roesler, S., Heinrich, W., Schraube, H., 2002. Monte Carlo calculation of the radiation field at aircraft altitudes. Radiat. Protect. Dosim. 98 (4), 367.
Rühm, W., Mares, V., Pioch, C., Weitzenegger, E., Vockenroth, R., Paretzke, H.G., 2009. Measurements of secondary neutrons from cosmic radiation with a Bonner sphere spectrometer at 79°N. Radiat. Environ. Biophys. 48, 125–133.
Rühm, W., Ackermann, U., Pioch, C., Mares, V., 2012. Spectral neutron flux oscillations of cosmic radiation on the Earth's surface. Geol. Geophys. Res. 117. A08309.
Rühm, W., Mares, V., Pioch, C., Agosteo, S., Endo, A., Ferrarini, M., Rakhno, I., Rollet, S., Satoh, D., Vincke, H., 2014. Comparison of bonner sphere responses calculated by different Monte Carlo codes at energies between 1 MeV and 1 GeV – potential impact on neutron dosimetry at energies higher than 20 MeV. Radiat. Meas. 67, 24–34.
Schraube, H., Jakes, J., Sannikov, A.V., Weitzenegger, E., Roesler, S., Heinrich, W., 1997. The cosmic ray induced neutron spectrum at the summit of the Zugspitze (2963 m). Radiat. Protect. Dosim. 70, 405–408.
Schraube, H., Mares, V., Roesler, S., Heinrich, W., 1999. Experimental verification and calculation of aviation route doses. Radiat. Protect. Dosim. 86 (4), 309–315.

Simmer, G., Mares, V., Weitzenegger, E., Rühm, W., 2010. Iterative unfolding for Bonner sphere spectrometers using the MSANDB code – sensitivity analysis and dose calculation. Radiat. Meas. 45, 1–9.

Usoskin, I., Alanko-Huotari, K., Gennady, A., Kovaltsov, G., Mursula, K., 2005. Heliospheric modulation of cosmic rays: monthly reconstruction for 1951–2004. Journal of Geophysical Research (Space Physics) 110. https://doi.org/10.1029/2005JA011250. A12108.

Wielunski, M., Brall, T., Dommert, M., Trinkl, T., Rühm, W., Mares, V., 2018. Electronic neutron dosimeter in high-energy neutron fields. Radiat. Meas. 114, 12–18.